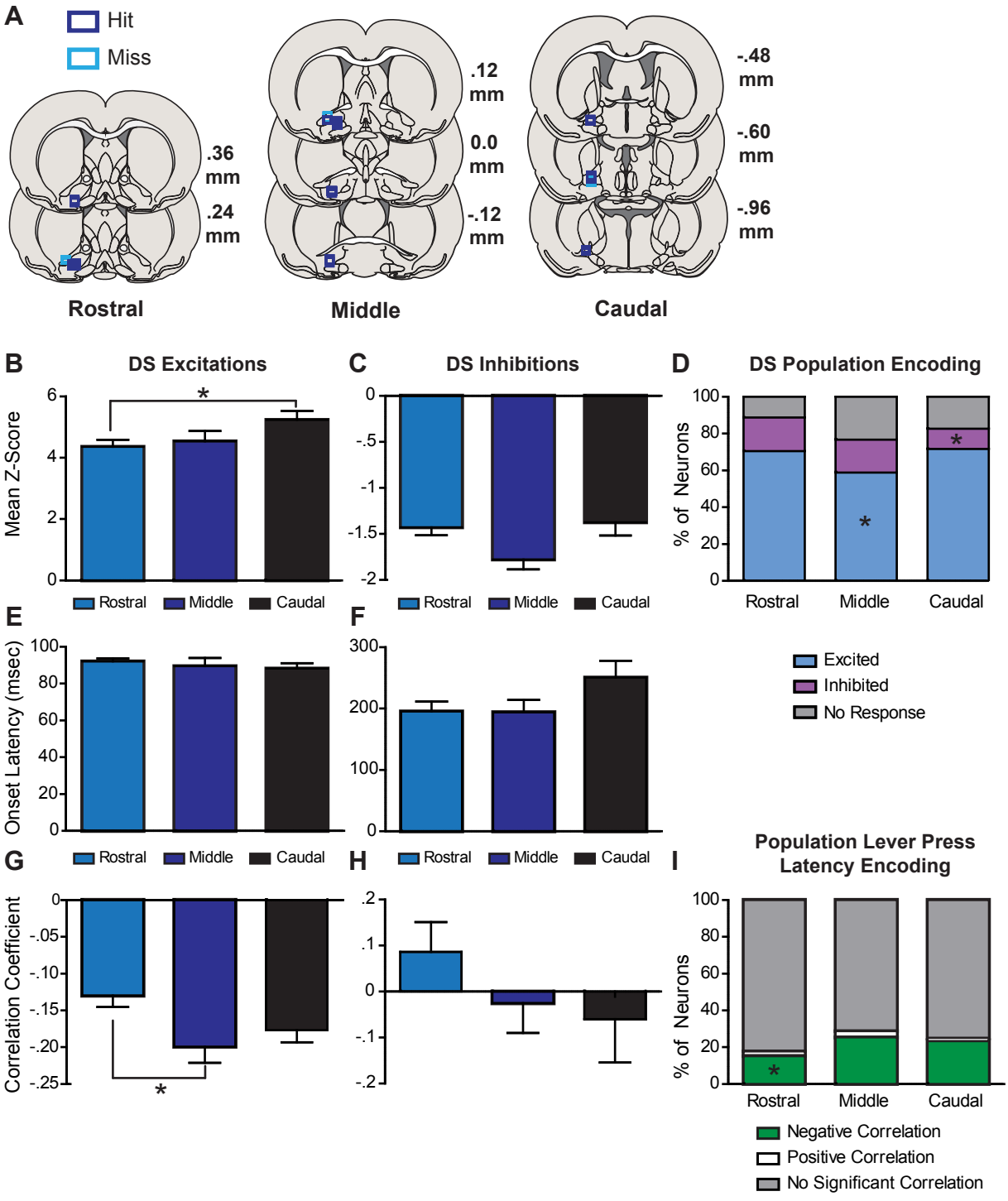
A
Hit
Miss
.36 mm
.24 mm
.12 mm
0.0 mm
-.12 mm
-.48 mm
-.60 mm
-.96 mm
Rostral
Middle
Caudal
B
DS Excitations
Mean Z-Score
C
DS Inhibitions
D
DS Population Encoding
% of Neurons
Excited
Inhibited
No Response
E
Onset Latency (msec)
F
G
Correlation Coefficient
H
I
Population Lever Press Latency Encoding
Negative Correlation
Positive Correlation
No Significant Correlation

Figure S1 (Refers to Figures 1 and 3). Histological localization of electrodes and rostrocaudal differences in response to the DS.

Because rostral and caudal VP neurons have different morphologic and electrophysiologic properties (Kupchik and Kalivas, 2013), and differentially modulate some reward-related behaviors (Johnson et al., 1993; Mahler et al., 2014; Smith and Berridge, 2005), we also looked for differences in encoding of the DS task in rostral (230 neurons), middle (146 neurons) and caudal (201 neurons) VP. Overall, encoding of the DS task by neurons is similar in rostral, middle and caudal VP. **A**, Reconstruction of electrode placements in rostral (left), middle (middle), and caudal (right) VP. Characteristics of DS-induced excitations (left) and inhibitions (middle) in terms of response magnitude (**B, C**, z-score), onset latency (**E, F**), and Spearman rank correlation coefficents relating firing and lever press latency (**G, H**) for recordings in rostral, middle and caudal VP. **D**, Proportion of neurons excited, inhibited or non-responsive in rostral, middle and caudal. **I** Proportion of neurons with negative, positive or no correlation between firing rate and DS response latency. *, $p<0.5$ subregion differences based Bonferroni's multiple comparisons or Chi-square tests. These results suggest that while middle VP neurons exhibit weaker population encoding of the DS, they more reliably encode the vigor of DS-induced reward seeking than more rostral VP neurons. Overall, the majority of neurons in each subregion were excited by the DS, and population activity in each subregion was predictive of behavioral response latency.

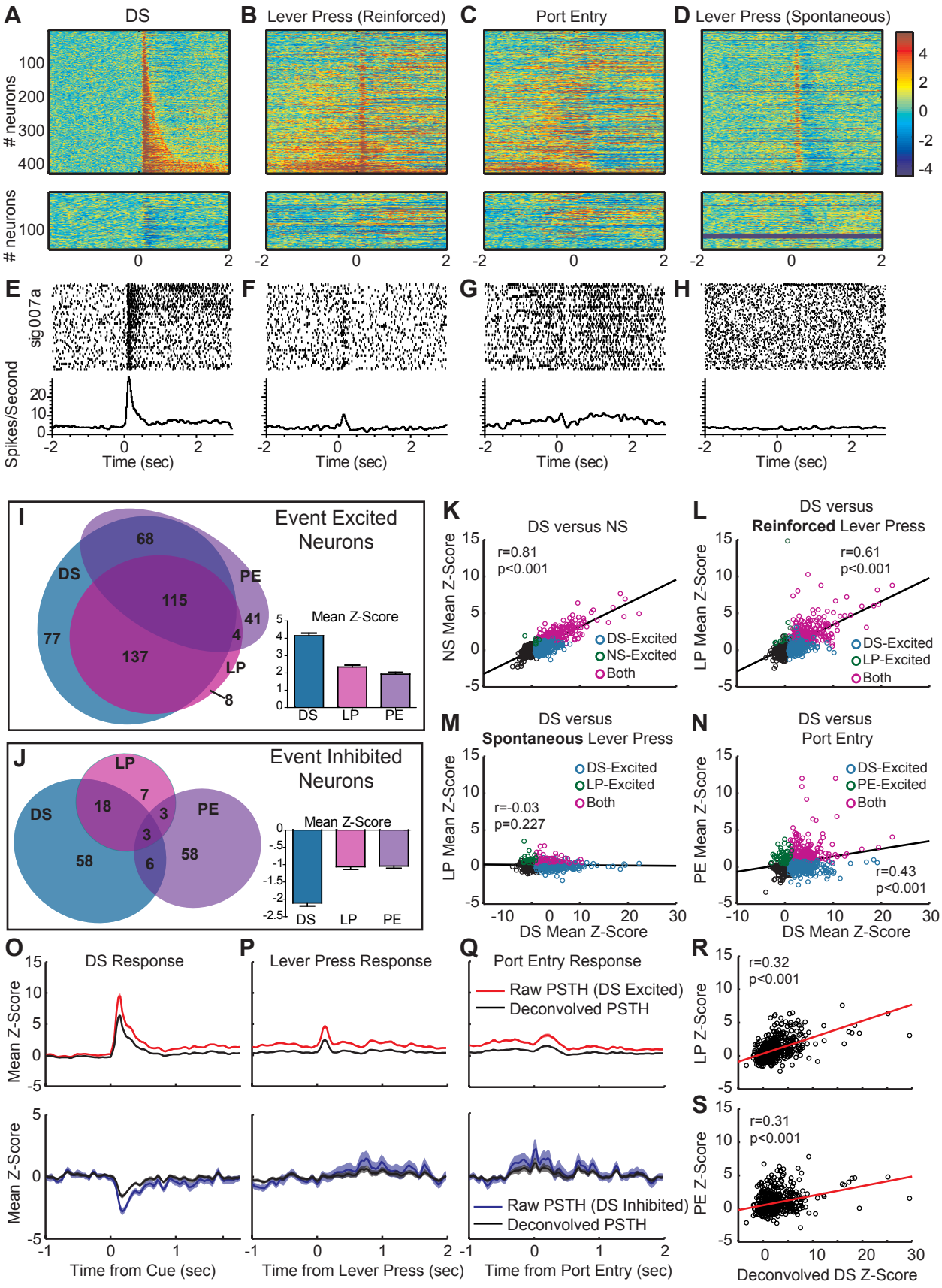
A
DS
B
Lever Press (Reinforced)
C
Port Entry
D
Lever Press (Spontaneous)
neurons
100
200
300
400
100
0
2
-2
4
2
0
-2
-4
E
F
G
H
sig007a
Spikes/Second
20
10
0
Time (sec)
I
Event Excited Neurons
68
DS
PE
115
41
4
77
137
LP
8
Mean Z-Score
DS
LP
PE
J
Event Inhibited Neurons
LP
7
18
3
DS
PE
3
58
6
58
K
DS versus NS
r=0.81
p<0.001
NS Mean Z-Score
DS-Excited
NS-Excited
Both
L
DS versus
Reinforced Lever Press
r=0.61
p<0.001
LP Mean Z-Score
DS-Excited
LP-Excited
Both
M
DS versus
Spontaneous Lever Press
r=-0.03
p=0.227
LP Mean Z-Score
DS-Excited
LP-Excited
Both
DS Mean Z-Score
N
DS versus
Port Entry
DS-Excited
PE-Excited
Both
r=0.43
p<0.001
PE Mean Z-Score
DS Mean Z-Score
O
DS Response
Mean Z-Score
Time from Cue (sec)
P
Lever Press Response
Time from Lever Press (sec)
Q
Port Entry Response
Raw PSTH (DS Excited)
Deconvolved PSTH
Raw PSTH (DS Inhibited)
Deconvolved PSTH
Time from Port Entry (sec)
R
r=0.32
p<0.001
LP Z-Score
S
r=0.31
p<0.001
PE Z-Score
Deconvolved DS Z-Score

Figure S2 (Refers to Figure 1). Relationship between VP neural responses to the DS and other task events.

Heat maps of responses to the DS (**A**), reinforced lever press (**B**), port entry (**C**), and spontaneous lever press (**D**) split into neurons in which we detected an initial excitation following the DS (top) and neurons in which we did not (bottom). Each line represents the PSTH of an individual neuron, -2 to 2 sec around the event of interest, normalized (z-score) and color-coded. Within each category, neurons are sorted by duration of response to the DS. Rasters (showing trial by trial firing) and correponding histograms show firing aligned to event onset in an example neuron for the DS (**E**), reinforced lever press (**F**), port entry (**G**) and spontaneous lever press (**H**). Venn diagrams illustrate the proportion of neurons that had significant responses to the DS, reinforced lever press (LP) and/or port entry (PE) when we compared firing during the analysis window to pre-DS firing, for neuron that showed increases in activity (Excited, **I**) and neurons that showed decreases in activity (Inhibited, **J**). The proportion of lever press-excited neurons that were also DS-excited far exceeded what one would expect from the proportion of the total population that was DS-excited (95% versus 68%; $X^2 = 71.514$, $p < 0.001$), and was significantly greater for the proportion of port entry-excited neurons as well (85% versus 68% using this text; $X^2 = 27.527$, $p < 0.001$ Insets show mean z-score for neurons responsive to each task event. Scatterplots of normalized mean event responses (z—scores) for the DS versus NS (**K**), DS versus reinforced lever press (**L**), DS versus spontaneous lever press (**M**) and DS versus port entry (**N)**, with each neuron represented as an individual circle, color-coded based on whether they significantly to the DS along (blue), the alternative event (green), both events (pink), or neither event (black). The magnitude of individual units' mean DS responses was most strongly related to their mean NS response, followed by the normalized response during reinforced lever presses (which coincide with DS termination and reinforcer delivery) and the response to port entry following reinforcer delivery. We found no correlation between the normalized response to spontaneous lever presses and the normalized DS response, suggesting that the DS response is not related to motor activity or action per se. We found no relationship between how neurons responded to the DS and how they responded to spontaneous lever presses. Units that had significant responses to the DS alone are marked in blue, units that had a response to the alternative event alone are marked in green, and those that responded to both are marked in pink. Because some correlations may arise due to the temporal proximity of task events and overlapping neural responses, we applied a deconvolution method described previously (Ghazizadeh et al., 2010) to isolate the contribution of each event to neural activity. Mean PSTHs are presented from raw (red, excited or purple, inhibited) and deconvolved data (black) from DS-excited (top) and DS-inhibited (bottom) neurons around the DS (**O**), reinforced lever press (**P**) and port entry (**Q**). Scatterplots illustrate the relationship between deconvolved DS responses and deconvolved activity during the lever press (**R**) and port entry (**S**). Following deconvolution these correlations were weaker, but still significant. This suggests that the processes that are represented by VP neural responses to the DS are represented weakly during other task events.

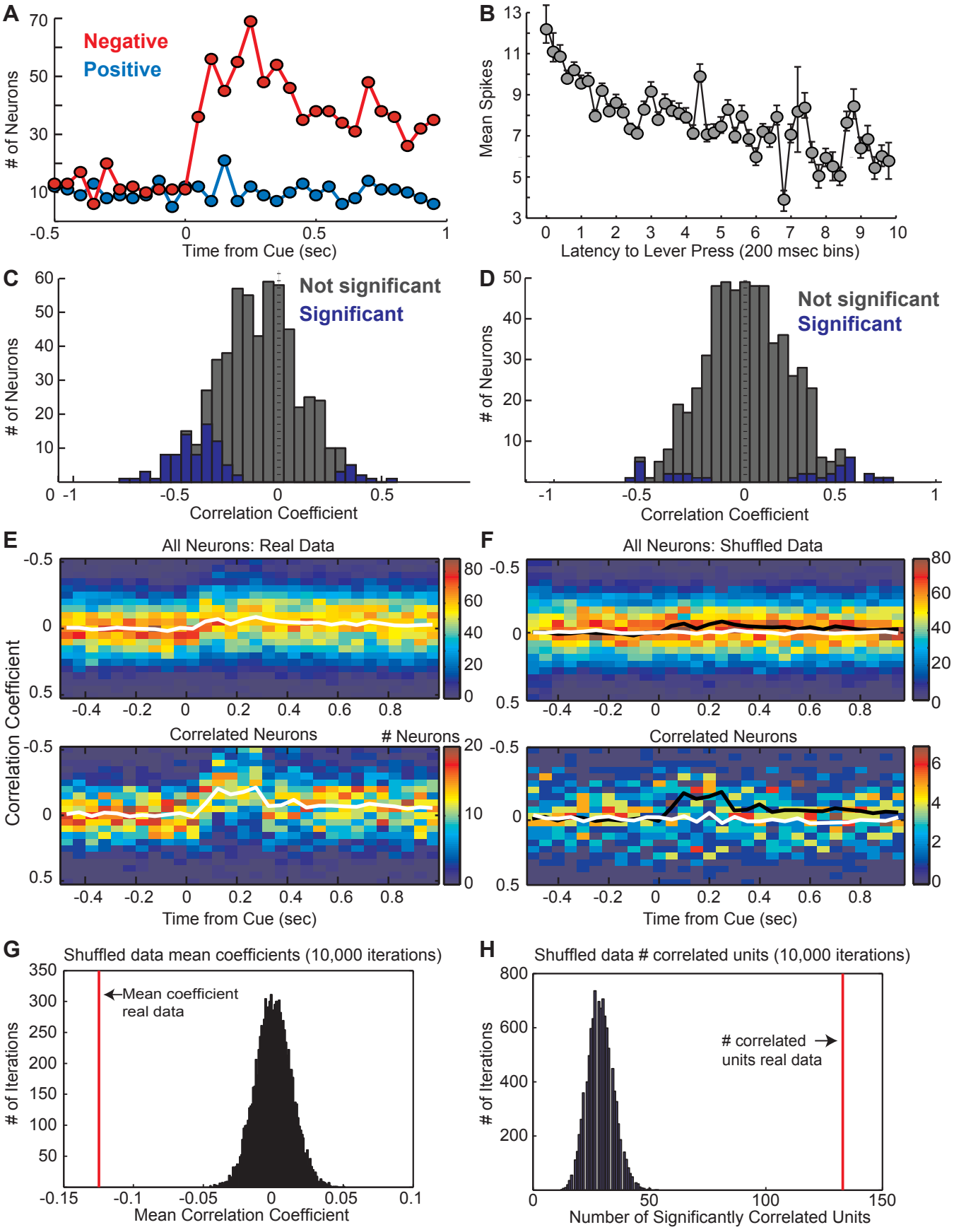
A
Negative
Positive
# of Neurons
Time from Cue (sec)
B
Mean Spikes
Latency to Lever Press (200 msec bins)
C
Not significant
Significant
# of Neurons
Correlation Coefficient
D
Not significant
Significant
# of Neurons
Correlation Coefficient
E
All Neurons: Real Data
Correlated Neurons
Neurons
Correlation Coefficient
Time from Cue (sec)
F
All Neurons: Shuffled Data
Correlated Neurons
Time from Cue (sec)
G
Shuffled data mean coefficients (10,000 iterations)
Mean coefficient real data
# of Iterations
Mean Correlation Coefficient
H
Shuffled data # correlated units (10,000 iterations)
correlated units real data
of Iterations
Number of Significantly Correlated Units

Figure S3 (Refers to Figure 3). Characterizing correlations between DS-evoked firing and response latency.

A) Number of neurons exhibiting negative (red) and positive (blue) correlations between firing rate and latency during 50 msec time bins around the DS (-.5 to 1 seconds). **B**) Mean spike # during the 90-300 msec analysis window based on latency to respond to the DS (latency averaged across 200 msec bins) with spike number averaged across the population (mean +/- SEM). **C**) Distribution of Spearman rank correlation coefficients relating firing during the inhibition analysis window (200-300 msec after DS onset) to the animal's latency to press the lever on a trial-by-trial basis. Bars shaded in purple show neurons with significant correlations, red line show median correlation coefficient for significant correlations. **D**) Example distribution of Spearman rank correlation coefficients from one iteration of the shuffled data, relating shuffled firing during the excitation analysis window (90-300 msec after DS onset) to the animal's latency to press the lever on a trial-by-trial basis. Bars shaded in purple show neurons with significant correlations. **E**) Distribution of Spearman rank correlation coefficients from the real data during 50 msec running windows around the DS (-.5 to 1 seconds), pooled into .05 size coefficient bins centered around zero, in all neurons (top) and in neurons with significant correlations (bottom). White lines indicate mean correlation coefficient in each window. **F**) Example distribution of Spearman rank correlation coefficients from one iteration of the shuffled data during 50 msec running windows around the DS (-.5 to 1 seconds), pooled into .05 size coefficient bins centered around zero, in all neurons (top) and in neurons with significant correlations (bottom). White lines indicate mean correlation coefficient of shuffled data and black lines indicate mean correlation coefficients from the real data. **G**) Distribution of mean Spearman correlation coefficients from 10,000 shuffled iterations of firing rate post-DS and latency on a trial-by-trial basis (black). The mean correlation coefficient from the real data is marked in red. **H**) Distribution of the number of significantly correlated units from 10,000 shuffled iterations of the data (the mean # of units is 5.03% of the data, for $p<0.05$). The number of significant Spearman correlation coefficients from the data is marked in red.

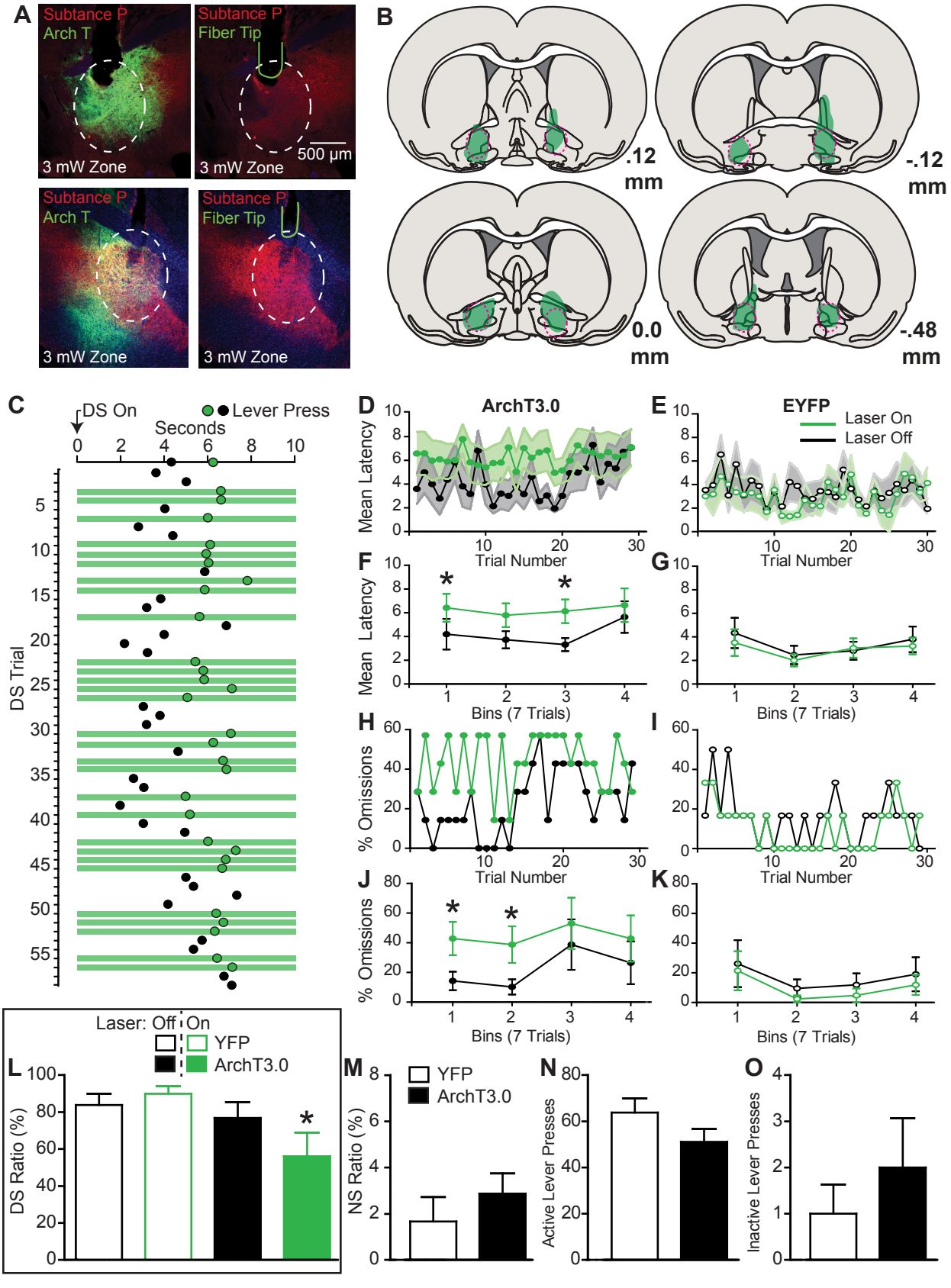
A
Subtance P
Arch T
3 mW Zone
Subtance P
Fiber Tip
500 µm
3 mW Zone
Subtance P
Arch T
3 mW Zone
Subtance P
Fiber Tip
3 mW Zone
B
.12 mm
-.12 mm
0.0 mm
-.48 mm
C
DS On
Lever Press
Seconds
0 2 4 6 8 10
DS Trial
5 10 15 20 25 30 35 40 45 50 55
D
ArchT3.0
Mean Latency
Trial Number
E
EYFP
Laser On
Laser Off
Trial Number
F
Mean Latency
Bins (7 Trials)
G
Bins (7 Trials)
H
% Omissions
Trial Number
I
Trial Number
J
% Omissions
Bins (7 Trials)
K
Bins (7 Trials)
L
Laser: Off On
YFP
ArchT3.0
DS Ratio (%)
M
YFP
ArchT3.0
NS Ratio (%)
N
Active Lever Presses
O
Inactive Lever Presses

Figure S4 (Refers to Figure 4). Virus localization and time course of effects of VP inhibition.

A, Examples of overlap between ArchT3.0 virus expression (green), the borders of VP as marked by immunostaining for substance P (red), and the estimated zone of >=3mW light intensity based on 10mW intensity of 532 nm light from a 300 micron fiber (Stujenske et al., 2015). **B**, Maximal spread of virus expression (green) at each rostrocaudal location where virus was expressed; pink circles represent the corresponding zone of >=3mW light intensity based on localization of fiber tips within these maximal virus expression zones. For each rat the overlapping zone of virus expression and 3mW light intensity was verified to be contained at least 80% within the borders of VP. Labels indicate anteroposterior distance from bregma (mm). **C**, Trial-by-trial average latency between DS onset (0) and lever press time (circles) on trials with laser on (green line and green circles) and no laser (black circles) in rats with ArchT3.0 virus expressed in VP. Average latency for each trial type is indicated on the top axis. Trial-by-trial latency with laser on (green) and no laser (black) trials in ArchT3.0 rats (**D**) and YFP control rats (**E**). Data presented are mean +/- SEM (shaded area). Average latency in bins of 7 trials for ArchT3.0 (**F**) and YFP control rats (**G**). Trial by trial % of omissions for ArchT3.0 (**H**) and YFP control rats (**I**). Average % of omissions in bins of 7 trials for ArchT3.0 (**J**) and YFP control rats (**K**). * = $p<0.05$ laser versus no laser. We did not find any significant effects of session bin (bins of 7 trials, interaction of bin x laser x virus: latency $F(3,33) = .644$, $p = .592$; response likelihood $F(3,33) = 1.062$, $p = .379$) or trial number (interaction of trial x laser x virus: latency $F(28,308) = 1.196$, $p = .231$; response likelihood $F(28,308) = .964$, $p = .522$) on the magnitude of changes induced by photoinhibition. Bar graphs illustrate percent of DS trials with a response (DS Ratio) on trials with the laser off (black) or on (green) in YFP (open) and ArchT3.0 (filled) rats (L), and for the YFP (open) and ArchT3.0 (filled) group the the percent of NS trials with a response (NS Ratio, **M**), the total number of active lever presses during the 2hr session (**N**) and the number of inactive lever presses during the 2 hr session (**O**). Graphs depict mean +/- SEM. *=$p<0.05$.

SUPPLEMENTAL EXPERIMENTAL PROCEDURES

Subjects

Male Long Evans rats (n=26; Harlan) weighing 250-275 grams at arrival were individually housed in a temperature- and humidity-controlled colony room on a 12 h light/dark cycle. After receipt, rats were allowed at least 1 week of *ad libitum* food and water. Starting one week prior to the initiation of training in the DS task, rats were food restricted to ~20g/rat/day, and the amount of food was adjusted daily in order to maintain rats at ~90% of their free feeding body weight. All experimental procedures were approved by the Institutional Animal Care and Use Committees at the University of California, San Francisco and at Johns Hopkins University and were carried out in accordance with the guidelines on animal care and use of the National Institutes of Health of the United States.

DS task training

Rats were trained to perform a DS task as described previously (Ghazizadeh et al., 2012). In the full version of the DS task, rats were placed in testing chambers with an "active" and an "inactive" lever, which were extended throughout the session. Rats in the pharmacological inactivation and electrophysiology experiments were assigned one of the following two auditory cues as their DS for training and testing: 1) an intermittent 4 kHz tone (40 ms on and 50 ms off) or 2) a siren tone (ramped from 4 to 8 kHz with a 400 ms period). Rats received the alternate cue as their NS. For the optogenetic inhibition experiment rats received a white noise or a 4 kHz tone as their DS, and received the alternative auditory cue as their NS. The DS and NS were presented on a pseudorandom variable interval schedule with a mean interval of 30 s, and each lasted up to 10 s. Presses on the active lever during the DS presentation resulted in liquid sucrose (10%) delivery and termination of the DS tone. Presses on the inactive lever, or on active lever during the NS presentation, had no programmed consequences. Rats were originally trained in the DS task daily for ~2 hours until they pressed the active lever during at least 60% of the DS presentations for the pharmacology experiment, and at least 80% of DS presentations for the electrophysiology and optogenetics experiments.

Surgeries

Rats received pre-surgical analgesia in the form of acetaminophen in their water bottles (4 mg/ml) starting 1 day prior to surgery. During surgery, rats were anesthetized with isoflurane (5%) and placed in a stereotaxic apparatus, after which surgical anesthesia was maintained with isoflurane (0.5-2.0%). Rats received injections of carprofen (5 mg/kg) and topical lidocaine for additional analgesia. Guide cannulae, electrodes, microdrives and fiberoptic implants were secured to the skull with bone screws and dental acrylic. Wire obturators were inserted into guide cannulae and were flush with the ends of the guide cannulae in order to avoid occlusion. All rats were given at least 7 days post-surgical recovery before beginning training or testing in the DS task.

Pharmacological inhibition: Rats used in the pharmacology experiment received cannulae implants after they had reached criteria in the DS task. Rats received bilateral 23 gauge guide cannulae aimed at the VP (n=7) using the following coordinates in comparison to bregma: 0.0 mm AP, +/- 2.3 mm ML, - 6.2 mm DV.

Electrophysiological recordings: After they had reached criteria in the DS task, rats in the VP electrophysiology experiment (n=6) received unilateral arrays of 16 electrodes each (0.004" tungsten wires arranged in bundles) attached to microdrive devices that allowed the entire array to be lowered by 80 or 160 µm increments. Electrode arrays were either targeted to rostral VP (n=3) at +0.35 mm AP, +1.8 mm ML, and -8.0 mm DV, or to caudal VP (n=3) at -0.35 mm AP, +2.5 mm ML, and -8.0 mm DV.

Optogenetic inhibition: Prior to the initiation of training in the DS task, rats in the optogenetic experiment received infusions of virus and optical fiber implants for optogenetic inhibition of VP (n=13). First, 0.7 µl of virus containing the archaerhodopsin gene construct (n=7; AAV5/CamKIIa-ArchT3.0-eYFP, $7x10^{12}$ viral particles/ml from the University of North Carolina Vector Core) or control virus (n=6; AAV5/CamKIIa-eYFP) was delivered bilaterally to VP through 28 gauge injectors at a rate of 0.1 µl per min for 5 minutes. Injectors were left in place for 10 min following the infusion to allow virus to diffuse away from the infusion site. Injector tips were aimed at the following coordinates in relation to Bregma: 0.0 mm AP, +/-2.5 mm mediolateral, -8.2 mm dorsoventral. Then, rats were implanted with 300 micron diameter optic fibers aimed .3 mm above the center of the virus infusion.

Pharmacological Inactivation of VP during the DS Task

In order to temporarily inactivate the VP we infused a mixture of the $GABA_A$ agonist muscimol and the $GABA_B$ agonist baclofen (10 ng each in .3 µl saline per side, infused at a rate of 0.3 µl per minute; Sigma). After

reaching criteria in the task (DS response ratio >60%), rats (n=7) received microinjections of vehicle prior to a final day of training, in order to habituate them to the testing procedure. Following each test day, rats received at least one day of drug-free retraining on the DS task, and were re-trained until the initial performance criteria were met before undergoing an additional test. To statistically assess the impact of baclofen-muscimol we used within-subject t-tests.

Electrophysiologal Recordings

Electrophysiological recording was conducted as described previously (Ambroggi et al., 2008; Ghazizadeh et al., 2010, 2012; Nicola et al., 2004). Rats were connected to the recording apparatus (Plexon Inc, TX), consisting of a head stage with operational amplifiers, cable and a commutator to allow free movement during recording. Rats were run for 2 hour daily sessions of the DS task, and recording was started after rats regained performance criteria (DS response ratio >80%) following surgery. The microdrive carrying the electrode arrays was lowered by 80 to 160 µm at the end of each session with satisfactory behavior (>60% of DS presentations with a response), in order to obtain a new set of neurons for each session that was included in the analysis.

Analysis of Electrophysiological Recordings

Spike sorting: Isolation of individual units was performed off-line with Offline Sorter (Plexon) using principal component analysis as described previously (Ambroggi et al., 2008; Ghazizadeh et al., 2012). Interspike interval distribution, cross-correlograms and autocorrelograms were used to ensure that single units were isolated. Only units with well-defined waveforms with characteristics that were constant over the entire recording session were included in the study. Sorted units were exported to NeuroExplorer 3.0 and Matlab for further analysis.

Determination of the optimal bin size: Optimal bin size was determined as described previously (Ambroggi et al., 2011; Ghazizadeh et al., 2012). Briefly, the optimal bin size for each neuron was found using Akaike Information Criteria (AIC). Because the optimal bin size is rather large for most neurons, and because the AIC shows a fast reduction over small bin sizes, followed by slow changes around the optimal bin size, we used the smallest possible bin size that showed less than a 10% change from the optimal AIC value. This bin size, referred to as the deflection point, was on average 49.5 msec across the population.

Response detection: Peri-stimulus time histograms (PSTHs), constructed around the behavioral events using the optimal bin size, were used to detect the presence of excitations and inhibitions, as well as their onsets and offsets, in comparison to a 10s baseline period prior to cue onset. At least one bin outside of the 99% confidence interval of the baseline during the analysis window for each event was required to determine an excitation or inhibition for that event. Onset detection was performed using a telescopic approach: within the first bin outside of the 99% confidence interval we searched for the first of three 10ms bin in which firing was beyond the 99% confidence interval of the baseline based on a 10ms bin size. This allowed us to determine onset times using the highest valid resolution for each PSTH. Response offset was found by finding the start of the first bin after the detected onset in which firing fell within the 99% confidence interval for at least 300 msec.

Data transformation, statistics and plotting: Based on detected response onset times, response direction was determined by running Wilcoxon sign-rank tests on firing during the 90 to 300 msec post-cue (excitations) or 200-300 msec post-cue (inhibitions) versus firing during the 10s baseline period. To compare firing in response to different task events (e.g. DS versus NS), Wilcoxon rank-sum tests were run on event related firing during these same windows. The firing rate of each neuron during each bin of the PSTH was transformed to a z-score as follows: $(F_i - F_{mean})/F_{sd}$, where F_i is the firing rate of the *i*th bin of the PSTH, and F_{mean} and F_{sd} are the mean and the SD of the firing rate during the 10s baseline period. Color-coded maps and average traces were constructed based on these z-scores.

Receiver operating characteristic (ROC) Analysis: To additionally assess the ability of VP neural firing to predict the presence or identity of cues and subsequent behavioral responses we conducted receiver operating characteristic (ROC) analysis evaluating 1) the DS response window in comparison to baseline, 2) the NS response window in comparison to baseline, 3) the DS window versus the NS window and 4) DS presentations that are followed by a lever press versus DS presentations not followed by a lever press. For each analysis we assessed the probability that firing during each window met criteria that ranged from zero to the maximum firing rate for that neuron, and plotted the true positive rate (likelihood that the firing in the window of interest was above criteria) versus the false positive rate (likelihood that the firing in the control window was above criteria) to create a ROC curve for each neuron. We then assessed the area under the ROC curve (auROC) for all VP neurons as well as the average ROC curve for the whole

population. We also conducted ROC analysis comparing two randomly selected baseline windows and then compared the test auROC distributions to this control auROC distribution. Finally, we identified the percentage of neurons for each analysis that had an auROC greater than 95% of auROCs in the control analysis (an auROC > 0.57).

Deconvolution Method: To tease apart the activity of events with relative temporal proximity we utilized a deconvolution method as described previously (Ambroggi et al., 2011; Ghazizadeh et al., 2010). Briefly, the model assumes that the total firing rate of a neuron in each trial is equal to the linear sum of the contributions of each event-related firing, delayed by the event latencies in that trial. Here, we deconvolved single event responses for each neuron using the maximum number of iterations that had a cross validation error lower than the PSTHs. We then used the average neural response for each event to assess relationships between activity during these events using Pearson correlations.

Correlation Analysis and Shuffled Data Controls: To assess the relationship between post-DS firing rate and latency to lever press in individual neurons, we ran Spearman's rank correlations. To assess the degree to which significant correlations occur spuriously in a small percentage of units, we ran Spearman correlations on 10,000 iterations of shuffled data. The trial-by-trial latency was randomly shuffled for each neuron for each iteration, and Spearman correlations related latency and firing rate during the 90-300ms post-DS window were assessed for each neuron. We then evaluated the distribution of both the number of units with significant correlations (at $p<0.05$) and the mean correlation coefficient, to confirm that both the mean correlation coefficient and the number of significant units from the real data was well outside the shuffled data distribution.

Optogenetic Inhibition

At least 4 weeks after surgery, and completion of training in the DS task (responses >60% of DS trials), rats with ArchT3.0-eYFP (n=7) or eYFP (n=6) rats were habituated to patch cord connections. Animals were connected via a ceramic mating sleeve to a 200 µm core patch cord, which was then connected through a fiber-optic rotary joint (Doric), to another patch cord which interfaced with a 532 nm DPSS laser. After at least 5 days of habituation to tethering during the task, rats were tested with continuous (10 sec) photoinhibition of VP (~20 mW light power) during 50% of DS presentations. Trials with and without photoinhibition were compared for latency to respond, and for the probability of a response. To statistically assess the effects of photoillumination in ArchT and control rats we used 2-way mixed ANOVAs (laser versus no laser, ArchT versus eYFP), followed by pairwise comparisons with Sidak corrections. To assess the impact of the VP photoillumination across time we used 2-way within-subject ANOVAs (laser versus no laser by trial or by bin [7 trials]) separately in ArchT and eYFP rats, followed by pairwise comparisons with Sidak corrections.

Histology

Animals were deeply anesthetized with pentobarbital and electrode sites were labeled by passing a DC current through each electrode. All rats were perfused intracardially with .9% saline following by 4% paraformaldehyde. Brains were removed, post-fixed in 4% paraformaldehyde for 4-24 hrs, cryoprotected in 25% sucrose for >48hrs, and sectioned at 50um on a microtome. For brains from electrophysiology or pharmacology rats, sections were stained with cresyl violet to locate injection or recording sites. The dorsoventral location of recording sites was determined by subtracting the distance driven between recording sessions from the final recording location. For brains from rats in the optogenetic experiments, we performed immunohistochemistry for GFP and/or substance P (SP), in order to identify the localization of virus expression and fiber placement within the borders of VP. Sections were washed in PBS with bovine serum albumin and triton (PBST) for 20 minutes, and incubated in 10% normal donkey serum in PBST for 30 minutes, before incubating in primary antibody (mouse anti-GFP 1:1500 Thermo Fisher #A11120, RRID: AB_10055152; rabbit anti-SP 1:6500 Immunostar #20064, RRID: AB_572266) in PBST overnight at room temperature. Sections were then washed with PBST 3-times, incubated in 2% normal donkey serum in PBS for 10 minutes, and incubated for 2 hours in secondary antibody in PBS (Alexa Fluor 488 donkey anti-mouse 1:200 Thermo Fisher #A21202, RRID: AB_10049285; Alexa Fluor 594 donkey anti-rabbit 1:500 Thermo Fisher #A21207, RRID: AB_10049744). Sections were then washed with PBS 3-times, mounted on coated glass slides in PBS, air-dried, and coverslipped with Vectashield mounting medium with DAPI.

SUPPLEMENTAL REFERENCES

Ghazizadeh, A., Fields, H.L., and Ambroggi, F. (2010). Isolating event-related neuronal responses by deconvolution. J. Neurophysiol. *104*, 1790–1802.

Ghazizadeh, A., Ambroggi, F., Odean, N., and Fields, H.L. (2012). Prefrontal cortex mediates extinction of responding by two distinct neural mechanisms in accumbens shell. J. Neurosci. *32*, 726–737.

Heidenreich, B., Mailman, R., Nichols, D., and Napier, T. (1995). Partial and full dopamine D1 agonists produce comparable increases in ventral pallidal neuronal activity: contribution of endogenous dopamine. J. Pharmacol. Exp. Ther. *273*, 516–525.

Johnson, P.I., Stellar, J.R., and Paul, A.D. (1993). Regional reward differences within the ventral pallidum are revealed by microinjections of a mu opiate receptor agonist. Neuropharmacology *32*, 1305–1314.

Mitchell, S.J., Richardson, R.T., Baker, F.H., and DeLong, M.R. (1987). The primate nucleus basalis of Meynert: neuronal activity related to a visuomotor tracking task. Exp. Brain Res. *68*, 506–515.

Smith, K.S., and Berridge, K.C. (2005). The ventral pallidum and hedonic reward: neurochemical maps of sucrose "liking" and food intake. J Neurosci *25*, 8637–8649.

Stujenske, J.M., Spellman, T., and Gordon, J.A. (2015). Modeling the Spatiotemporal Dynamics of Light and Heat Propagation for In Vivo Optogenetics. Cell Rep. *12*, 525–534.

Tachibana, Y., and Hikosaka, O. (2012). The primate ventral pallidum encodes expected reward value and regulates motor action. Neuron *76*, 826–837.